

Simulation of Glassy State Relaxations in Polymers: Prediction of the Dielectric Loss Spectrum Due to Methoxy Group Rotation in Poly(vinyl methyl ether)

Jean-Claude Berthet[†] and Geoffrey R. Davies^{*,‡}

Science Institute VR2, University of Iceland, IS-107 Reykjavik, Iceland, and Polymer IRC, School of Physics, University of Leeds, Leeds LS2 9JT, United Kingdom

Received September 4, 2006; Revised Manuscript Received March 22, 2007

ABSTRACT: In this paper, we show that it is possible to predict the dielectric loss spectrum of methoxy groups in amorphous poly(vinyl methyl ether) from their rotational energy profiles obtained by a simple quasistatic technique described in our previous paper. Kramers' transition rate theory is used with a slight modification to account for the nonquadratic profiles encountered and short molecular dynamics runs are used to obtain the moment of inertia and rotational frictional coefficient of a methoxy group. The predicted dielectric loss spectrum and its temperature dependence are in good agreement with experimental observations with no adjustable parameters other than those specified in the force field. It is found that the width of the dielectric loss spectrum is essentially due to the spread of activation energies with a negligible contribution from the spread of relaxation time prefactors.

1. Introduction

Relaxations in polymers in the glassy state generally occur far too slowly for direct simulation by molecular dynamics techniques. We have shown in a previous publication¹ that the quasistatic technique may be used to determine the energy profile for the rotation of methyl and methoxy groups in poly(vinyl methyl ether) (PVME) and that the method gives good agreement with the observed dielectric increment of PVME conventionally assigned to the rotation of the methoxy groups. The average activation energy, however, was determined by an ad hoc averaging procedure rather than by analyzing the shift in dielectric loss with frequency as is done experimentally. In this paper, we present a method for determining the frequency dependence of the dielectric loss from the simulated rotation energy profiles of the methoxy groups and analyze the temperature dependence of the loss process in a similar manner to the experimentalists to generate an activation energy and rate prefactor for direct comparison with experimental results.

The methoxy group rotational energy profiles are generally similar to that shown in Figure 1, with two minima in a complete rotation centered around 0° and ±180°. Transitions between these minima can occur in either the clockwise or anticlockwise direction with, in general, two different barriers. In our previous paper,¹ we discussed the use of both two-site and three-site models (where the 180° minimum reached by a clockwise rotation was treated as a different state to that reached by an anticlockwise rotation), but in this paper, we consider only the two-site model. A further simplification is to neglect any local field treatment because, as shown in our previous paper,¹ only a small fraction of the groups actually make a significant contribution to the dielectric response, and hence dipolar correlations can be neglected because we are dealing with an effectively dilute dipolar system. With these simplifications, each rotating methoxy group can be considered as generating a single Debye relaxation with relaxation parameters that depend upon

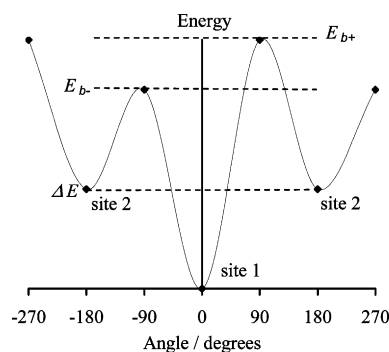


Figure 1. Two-site model with two barriers.

its energy profile, which is determined, in part, by the group's local environment.

Given the energy profiles from our previous paper,¹ our first task in this paper is to determine the transition rates between the two sites. This requires a detailed investigation of transition rate theories to determine which is most appropriate. Once the transition rates are calculated, the frequency and temperature dependence of the permittivity is readily obtained. The shift in the dielectric loss with temperature is then analyzed in a similar manner to the experimental studies to yield a mean activation energy and a spread of activation energies for comparison with experiment.

2. Theory

2.1. Two-Site Model. The model used is a modified version of the two-site model published by Hoffman and Pfeiffer.² In the problem considered here, four transitions are possible because forward and backward transitions may be made in a clockwise or anticlockwise direction. We denote the rates of the transitions by v_{1b+2} , v_{1b-2} , v_{2b+1} , and v_{2b-1} . The first two rates are the probabilities per unit of time to jump from site 1 to site 2 over the two different barriers, while the second two are the probabilities per unit of time to jump from site 2 back to site 1. The $b+$ and $b-$ subscripts indicate over which of the two barriers the transition occurs. The rate equations for this model are:

* To whom correspondence should be addressed. E-mail: g.r.davies@leeds.ac.uk.

[†] Science Institute VR2, University of Iceland.

[‡] Polymer IRC, School of Physics, University of Leeds.

$$\frac{dN_1}{dt} = -(v_{1b+2} + v_{1b-2})N_1 + (v_{2b+1} + v_{2b-1})N_2 \quad (1)$$

$$\frac{dN_2}{dt} = +(v_{1b+2} + v_{1b-2})N_1 - (v_{2b+1} + v_{2b-1})N_2 \quad (2)$$

where N_1 and N_2 are the fraction of groups in site 1 or 2, respectively. Normalization implies that:

$$N_1 + N_2 = 1 \quad (3)$$

After a perturbation, the population difference, $\Delta N (= N_1 - N_2)$ decays exponentially with a relaxation time τ given by:

$$\frac{1}{\tau} = \nu = v_{1b+2} + v_{1b-2} + v_{2b+1} + v_{2b-1} \quad (4)$$

The change in dipole moment is driven by this population difference and hence has the same relaxation time. Determination of τ thus requires the calculation of the transition rates from the barrier profiles.

2.2. Calculation of Transition Rates. There is no general solution for the evaluation of the transition rates from the barrier profiles. The equations and theorems presented below have been developed and published by several authors over the last century, as is well summarized by Hänggi, Talkner and Borkovec.³ We considered three different models:

1. Transition State Theory (TST). In its one-dimensional version,³ this is easy to apply. It can be solved exactly by integrating the energy profile, and approximations can be avoided with no need to fit the curvature of the well. It requires only the moment of inertia of the rotating group with no friction coefficient.

2. Smoluchowski's Model. This is a little more complicated than TST. The one-dimensional version³ can also be solved exactly, but it requires a double integration over the energy profile. Because it assumes high friction, it requires knowledge of the friction coefficient but not the moment of inertia.

3. Kramers' Model for Intermediate-to-Strong Friction. This cannot be solved by integrations of the energy profile. The standard solution³ assumes that the maxima and minima in the energy profiles are quadratic within a range of several kT , and it requires values for both the moment of inertia and friction coefficient.

Exploratory studies of the methoxy groups' librational motions within their wells by molecular dynamics techniques showed that their motion was not well-described by either the low-friction or high-friction regime, and hence Kramers' model should be used. Unfortunately, the extrema in the rotational energy profiles were not well fitted by a quadratic approximation, especially the 0° minimum. We therefore developed an alternative fitting protocol to derive the effective curvatures by applying the TST and Smoluchowski models as described below.

2.3. Transition State Theory. The Hamiltonian for a methoxy group is assumed to be:

$$H(L, \varphi) = \frac{L^2}{2I} + E(\varphi) \quad (5)$$

The letters φ and L are the methoxy group's dihedral angle and corresponding angular momentum. I is its moment of inertia and $E(\varphi)$ is the potential energy as a function of dihedral angle determined by QS simulations.

The TST rate of escape is given by:

$$v_{\text{TST}} = \frac{\sqrt{\frac{k_B T}{2\pi I}} \exp\left(-\frac{E_{\text{Max}}}{k_B T}\right)}{Z_\varphi} \quad (6)$$

where Z_φ is given by:

$$Z_\varphi = \int_{b_-}^{b_+} d\varphi \exp\left(-\frac{E(\varphi)}{k_B T}\right) \quad (7)$$

and E_{Max} is the energy of the barrier across which the system escapes. Z_φ is integrated between the two barriers delimiting the well from which the system is escaping. Note that the minimum energy of the well does not need to be subtracted from the maximum energy E_{Max} because it will be removed by the normalization Z_φ .

In the Gaussian approximation, eq 6 becomes an Arrhenius equation:

$$v_{\text{TST}} = \frac{\omega_0}{2\pi} \exp\left(-\frac{E_b}{kT}\right) \quad (8)$$

where ω_0 is the angular frequency of the system in the bottom of the well and E_b is the energy barrier (i.e., $E_{\text{Max}} - E_{\text{Min}}$).

2.3.1. The Smoluchowski Limit. The Smoluchowski escape rate for a nonquadratic potential, within the steepest descent approximation, is:

$$v_{\text{Smo}}^{-1} = \frac{\zeta}{k_B T} \int_{\text{Min}1}^{\text{Min}2} dy \exp\left(\frac{E(y)}{k_B T}\right) \int_{\text{Max}1}^{\text{Max}2} dx \exp\left(-\frac{E(x)}{k_B T}\right) \quad (9)$$

This is valid when friction is so strong that inertial effects can be ignored. Equation 9 does not require a mass or moment of inertia, but it requires a friction coefficient ζ . In the Gaussian approximation, eq 9 becomes:

$$v_{\text{Smo}} = \frac{I\omega_0\omega_b}{2\pi\zeta} \exp\left(-\frac{E_b}{kT}\right) \quad (10)$$

where ω_0 is the angular frequency of the system in the bottom of the well and ω_b is the effective angular frequency of the system at the top of the barrier if the sign of the curvature were changed.

2.3.2. Kramers' Intermediate and High Friction Limit. Kramers' model uses both a moment of inertia and a friction coefficient and assumes that the extrema may be adequately represented by quadratic representation over a range of several kT in energy. The solution for the transition rate is then:

$$v_{\text{Kramer}} = \left[\sqrt{1 + \left(\frac{\zeta}{2\omega_b I}\right)^2} - \frac{\zeta}{2\omega_b I} \right] \frac{\omega_0}{2\pi} \exp\left(-\frac{E_b}{kT}\right) \quad (11)$$

In the limit of a negligible friction coefficient, Kramers' expression becomes the TST expression, while for high friction, it becomes the Smoluchowski expression.

The parameters ω_0 and ω_b are usually determined by fitting parabolas to $E(\varphi)$ in the region of the extrema and then computing ω_0 and ω_b . In our case, however, we found that the potentials could not be adequately represented by a quadratic form over the necessary range of energies, and we therefore adopted an alternative approach to determine ω_0 and ω_b from $E(\varphi)$. In the Gaussian approximation, we have the relation:

$$\frac{v_{\text{TST}}}{2v_{\text{Smo}}} = \frac{\zeta}{2\omega_b I} \quad (12)$$

Kramers' escape rate can be rewritten as a function of v_{Smo} and v_{TST} only.

$$v_{\text{Kramer}} = \left[\sqrt{\left(\frac{v_{\text{TST}}}{2v_{\text{Smo}}} \right)^2 + 1} - \frac{v_{\text{TST}}}{2v_{\text{Smo}}} \right] v_{\text{TST}} \quad (13)$$

Instead of fitting the energy profile with quadratic polynomials, we utilized the integrated versions of the TST and Smoluchowski rate equations (6 and 9) to determine v_{Smo} and v_{TST} by integration over the energy profile and thus free ourselves from the quadratic approximation.

2.3.3. Determination of the Moment of Inertia and Friction Coefficient. The effective moment of inertia and effective friction coefficient were determined by MD simulation. To ensure simple analysis of the trajectories, a quadratic forcing potential of 20 kcal mol⁻¹ rad⁻² was added to the torsional angle of the five most dielectrically active groups. This forcing potential had two effects: primarily, because it is quadratic and strong compared to the natural potential, it reduced the effects of the nonquadratic potential and ensured that a simple analysis could be performed; second, it also reduced the effects of the friction (see eq 15), assuring that we were in an underdamped, oscillating regime that allowed good fits to be obtained.

The dihedral angle autocorrelation function was analyzed by assuming that the moment of inertia and frictional coefficient were constant and that the equation of rotational motion was adequately represented by:

$$I\ddot{\varphi} + \zeta\dot{\varphi} + 2k\varphi = 0 \quad (14)$$

where φ is the dihedral angle, I is the moment of inertia, ζ is the friction coefficient, and $2k\varphi$ is the restoring force from the forcing potential, $E = k(\varphi - \varphi_{\text{min}})^2$.

The relative effects of friction and inertia can be described by the parameter Δ .

$$\Delta \equiv \frac{\zeta^2}{8Ik} \quad (15)$$

If $\Delta < 1$, then the system is oscillatory and the autocorrelation function has the form:

$$\phi(t) = \exp\left(-\frac{t}{\tau}\right) \cos(\omega t) \quad (16)$$

The parameters τ and ω are determined by fitting the autocorrelation function. With the parameters τ , ω , and k known, the moment of inertia, I , and the friction coefficient, ζ , can be calculated from:

$$I = \frac{2k}{\omega^2 + \frac{1}{\tau^2}} \quad (17)$$

$$\zeta = \frac{4k\tau}{1 + (\omega\tau)^2} \quad (18)$$

An alternative fitting method based on the Fourier transform was also used.

$$\text{FT}_{\varphi}(p) = \frac{1}{\sqrt{2\pi}} \int_{-\infty}^{+\infty} \varphi(t) \exp(-ipt) dt \quad (19)$$

The correlation functions $\phi(t)$ were defined as null for $t < 0$. In that case, the Fourier transform of eq 16 gives a real and imaginary part:

$$\text{Re}[\text{FT}_{\phi}] = \frac{1}{2\sqrt{2\pi}} \left\{ \frac{\nu}{\nu^2 + (p - \omega)^2} + \frac{\nu}{\nu^2 + (p + \omega)^2} \right\} \quad (20)$$

$$\text{Im}[\text{FT}_{\phi}] = \frac{1}{2\sqrt{2\pi}} \left\{ \frac{\omega - p}{\nu^2 + (p - \omega)^2} - \frac{\omega + p}{\nu^2 + (p + \omega)^2} \right\} \quad (21)$$

where $\nu = 1/\tau$. The complex Fourier transform of the correlation function found by simulations was fitted with the two functions in eqs 20 and 21, and the moment of inertia and the friction coefficient of the methoxy group were then obtained from eqs 17 and 18.

2.4. Calculation of Dielectric Relaxation Parameters. We assume that any individual methoxy group in a glassy environment undergoes simple Debye relaxation with a relaxation time τ that differs from group to group. The permittivity for the whole polymer is obtained by summation of the contributions from each group. The real part of the permittivity is thus given by:

$$\epsilon'(\omega) = \sum_i \Delta\epsilon_i \frac{1}{1 + (\omega\tau_i)^2} + \epsilon(\infty) \quad (22)$$

and the imaginary part by:

$$\epsilon''(\omega) = \sum_i \Delta\epsilon_i \frac{\omega\tau_i}{1 + (\omega\tau_i)^2} \quad (23)$$

where ω is the imposed angular frequency of measurement, $\epsilon(\infty)$ is the permittivity at high frequency, i is a group index (the summations are performed over all groups), and the i th group is characterized by two parameters $\Delta\epsilon_i$ and τ_i , which are its dielectric increment and relaxation time, respectively. It is these final two parameters that need to be determined from the QS simulation data.

The dielectric increment resulting from a static analysis was given in our previous paper¹ as:

$$\Delta\epsilon_i = \frac{\langle (\mu_i - \langle \mu_i \rangle)^2 \rangle}{3k_B T V \epsilon_0} \quad (24)$$

where μ_i is the vector dipole moment of the i th group and the angular brackets denote ensemble averaging.

In our previous static analysis, μ_i was simply taken as the dipole moment at the minimum energy within a well. In this analysis, however, because the relaxation time is determined from integration over the energy profile, it is consistent to use the average dipole moment within the well defined by:

$$\bar{\mu} = \int_{\text{max1}}^{\text{max2}} \mu(\varphi) \exp\left(\frac{-E(\varphi)}{k_B T}\right) d\varphi \quad (25)$$

where μ is the dipole moment at a certain dihedral angle φ and the integration is performed over all the space between two energy maxima (or barriers) defining the limits of the well.

In our previous paper,¹ we discussed whether the wells reached by positive and negative rotations of 180° should be considered the same site. If they are considered as different, due to different changes occurring in the environment for example, then wells accessed by further rotations should

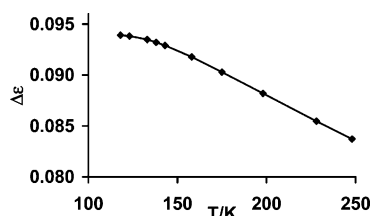


Figure 2. Total simulated dielectric relaxation strength as a function of the temperature.

logically also be considered different. We do not have data for rotations starting from these new states, and consequently, for the dynamic analysis presented in this paper, we are forced to assume that rotations of $+180^\circ$ or -180° from the initial well access the same new well and that rotations from the new well return to the original well. We thus consider only a two-site model. All average site properties such as occupancy, mean dipole moment, mean square dipole moment, etc., are then obtained by Boltzmann-weighted integrations similar to eq 25 taken over the appropriate well.

To perform the ensemble averages, a weight needs to be attributed to each site. This weight is the local partition function:

$$Z = \int_{\max 1}^{\max 2} d\varphi \exp\left(-\frac{E(\varphi)}{k_B T}\right) \quad (26)$$

We then have for each dipole four parameters: μ_0 , μ_{180} , the two average dipoles defined by eq 25 and Z_0 , and Z_{180} , the two non-normalized occupancy probabilities attributed to the wells. The two-site ensemble averages can then be performed in accordance with:

$$\langle f \rangle = \frac{Z_0 f_0 + Z_{180} f_{180}}{Z_0 + Z_{180}} \quad (27)$$

where f stands for any relevant value such as μ , μ^2 , or $\mu - \langle \mu \rangle$, etc.

3. Application and Results

The QS profiles used were those from the “limited” simulation in our previous paper.¹ That is, the 30 most dielectrically active groups from each of the six cells whose energy profiles were reanalyzed under the least computationally restrictive minimization conditions. Application of the protocol described in Section 2.4 to calculate the overall relaxation strength from these profiles yields the result shown in Figure 2.

The calculated value of the relaxation strength at 138 K is 0.093, which is slightly less than the value of 0.096 derived in our previous publication,¹ which was calculated from the properties at the well minima rather than averaging over the well profile.

To generate dynamic data, we need to know the moment of inertia and friction coefficient for methoxy group rotation. These data were obtained for the five most dielectrically active groups from molecular dynamics simulations run at a temperature of 150 K for 10 ps with the extra quadratic potential added to the dihedral energy term as described above. Ten runs were done on each group, and the average angular correlation function for each group was calculated. No temperature control algorithm was used to avoid artificial changes in the motion of the atoms brought about by the action of a thermostat. The strength of the forcing potential (set by k) was checked by running a 2 ns molecular dynamics in the same condition and analyzing the

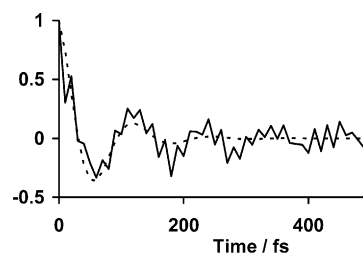


Figure 3. Example of a librational angle correlation function at 150 K. Solid line: data; dotted line: fit.

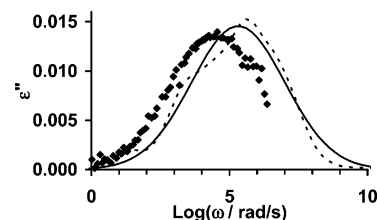


Figure 4. ϵ'' as a function of frequency at 138 K. Squares: experiment⁵ with a baseline loss of 0.00712 removed (see text below). Dotted line: simulation. Continuous line: RRDM fit to simulation.

Table 1. Moments of Inertia, I , in kcal mol⁻¹ degree⁻² fs², Friction Coefficients, ζ , in kcal mol⁻¹ deg⁻² fs², and Values of Δ Found for Each of the Five Groups by the Two Different Fitting Methods

minimum	time correlation function			Fourier transform		
	I	z	D	I	z	D
$\sim 0^\circ$	5.48	0.25	1.61	5.49	0.25	1.58
$\sim 180^\circ$	6.23	0.21	0.32	6.23	0.21	0.31
$\sim 0^\circ$	6.46	0.21	1.06	6.48	0.21	1.05
$\sim 0^\circ$	6.18	0.18	0.54	6.19	0.18	0.53
$\sim 0^\circ$	8.19	0.16	0.18	8.21	0.16	0.17
average	6.51	0.20	0.74	6.52	0.20	0.73
std deviation	1.01	0.03	0.59	1.01	0.03	0.58
error	0.45	0.02	0.26	0.45	0.02	0.26

probability of observing a given dihedral angle. A typical angular autocorrelation function is shown in Figure 3.

The moment of inertia and friction coefficients for each of the five groups were found by directly fitting the angular autocorrelation functions as described above. The same parameters were also determined by fitting a discrete Fourier transform of the correlation function with the appropriate normalization to obtain the Fourier transform as defined by eq 19. Both methods give similar results with similar errors as shown in Table 1. Note that the values of Δ confirm that we are generally in the intermediate friction limit.

The average values for the mass and the friction coefficients given in Table 1 were used for all units in the subsequent analysis. Unfortunately, we have not investigated if these values depend upon the strength of the forcing potential used to obtain them. Note, however, that highly accurate values are not required because an error of a factor of 2 in moment of inertia for example will only change the logarithm of τ_0 in eq 28 by 0.15, while $\text{Log } \tau_0$ is 12.6 and the width of the relaxation peak is 4 decades. An error of two standard deviations in moment of inertia would change $\text{Log } \tau_0$ by only about 0.05.

3.1. Reconstructed Loss Peak and RRDM Fit. For each group, the four escape rates were calculated using Kramers' model for intermediate and strong frictions (eq 13). The relaxation time was determined from eq 4 and the relaxation strength from eq 24. Then, summing the contributions from each group (eq 23) yielded the dielectric loss curve associated with methoxy group rotation (dotted line in Figure 4). These data were calculated at 138 K for comparison with the experimental curve reported at this temperature.

Table 2. Quantitative Comparison between Experiment and Simulation

	$\Delta\epsilon$	E_0 kJ/mol	σ_E kJ/mol	$\log(\tau_0/s)$
expt Cendoya et al.	0.120	21.70	4.90	
expt Gomez et al.	0.086	21.23	4.25	12.59
simulation	0.085	19.29	4.01	12.62

The simulation result is not a smooth peak because it is dominated by the contributions from a few units. Nevertheless, the comparison with experiment is impressive, especially when one considers that the simulation data come directly from the force field with no arbitrarily adjustable parameters. The simulated loss peak height and width are comparable with the experimental data, and the error in the position of the loss peak is substantially less than the peak width.

To make a quantitative comparison, we note that the experimental data were analyzed using the rotational rate distribution model (RRDM). In this model, the relaxation time, τ , is written as a function of the activation energy, E , as a simple Arrhenius expression:

$$\tau(E) = \tau_0 e^{(E/T)} \quad (28)$$

where the parameter τ_0 is assumed constant. The relaxation strength is assumed to be a Gaussian function of the activation energy such that the real and imaginary parts of the permittivity can be written:

$$\epsilon(\omega) - \epsilon_\infty = \frac{\Delta\epsilon}{\sqrt{2\pi}\sigma_E} \int_{-\infty}^{+\infty} \exp\left(-\frac{(E - E_0)^2}{2\sigma_E^2}\right) \times \frac{dE}{1 + i\omega\tau(E)} \quad (29)$$

$$\epsilon''(\omega) = \frac{\Delta\epsilon}{\sqrt{2\pi}\sigma_E} \int_{-\infty}^{+\infty} \exp\left(-\frac{(E - E_0)^2}{2\sigma_E^2}\right) \times \frac{\omega\tau(E) dE}{1 + i\omega\tau(E)} \quad (30)$$

The model thus has four fitting parameters: $\Delta\epsilon$, the total dielectric increment, τ_0 , the relaxation time prefactor, E_0 , the most probable activation energy, and σ_E , which describes the width of the distribution of activation energies. These cannot all be determined from data at a single temperature, hence the loss curve was fitted at 138 and 248 K with the same four parameters. The results are summarized in Table 2.

It can be seen that experimental and simulated data, all analyzed by the RRDM method, yield results that are in excellent agreement. The mean activation energy of 19.3 kJ/mol from RRDM analysis is an improvement on our previous simply weighted result of 18.3 kJ/mol, bringing us closer to the observed values of 21.2 and 21.7 kJ/mol. There is obviously a discrepancy in the quoted experimental relaxation strength, but we are in close (certainly somewhat fortuitous) agreement with the Gomez⁴ result while we differ somewhat from the Cendoya⁴ result. Our width parameter, σ_E , also agrees better with the Gomez⁴ result.

The relaxation strength for the data of Gomez et al.⁴ was not quoted in their publication. We have therefore refitted their data at 138 K with the RRDM expression plus an additional flat background loss as described by them. For comparison with our simulation, their experimental data shown in Figure 4 have had a background loss level removed. Consequently, the loss attributed to the methoxy group rotation is reduced, and the total relaxation strength calculated from the RRDM fit is in good agreement with our calculations.

Cendoya et al.⁵ mention that they assumed a polynomial functional form for the background loss but do not quote the

parameters or even the degree of polynomial used. If their background loss subtraction does not remove as much loss from the data, then this would account for the different relaxation strength found by them.

3.2. The Distribution of Relaxation Time Prefactors. The RRDM assumes a constant prefactor, τ_0 , for all groups. The width of the distribution of relaxation times in this model thus arises solely from the different activation energies of the groups. It was felt to be important to check the validity of this hypothesis. We therefore calculated the barrier crossing rates for every group at 150 and 175 K and, assuming the validity of eq 28, calculated E and τ_0 for each group from these data. The simple average value of $\log(\tau_0/s)$ was found to be 12.68, and the distribution had a surprisingly small standard deviation of 0.17. This is not the whole story, however, because the simple average activation energy is only 10.9 kJ/mol, which is far from reality (~ 21 kJ/mol). As discussed in our previous paper,¹ it is necessary to take a weighted average where the weights reflect the dielectric strength of each group to obtain something near the observed activation energy. We therefore weighted the calculation of $\log(\tau_0/s)$ with the same weights to obtain a weighted average $\log(\tau_0/s)$ of 12.86, while the standard deviation narrowed to 0.10 or one-tenth of a decade. Because the width of a single Debye process is 1.12 decades, the assumption of a constant prefactor is well justified by our simulation data.

In passing, we note that the variation in $\log(\tau_0/s)$ that does occur tends to be correlated with the activation energy. Writing

$$\text{Log}(\tau_0/s) = -(aE + b) \quad (31)$$

an unweighted fit yields $a = 0.020$ (kJ/mol)⁻¹ and $b = 12.46$, while a weighted fit yields $a = 0.010$ (kJ/mol)⁻¹ and $b = 12.66$.

4. Conclusion

The dielectric loss associated with the β relaxation in PVME can be predicted by combining QS determination of rotational energy profiles of methoxy groups with MD simulations to obtain their moment of inertia and friction coefficient. The final dielectric loss spectrum has no adjustable parameters, other than those in the forcefield itself, and is in excellent agreement with experiment.

The rotational rate distribution model, applied to both experimental and simulated data, gives similar values for the relaxation time prefactor, activation energy, and spread of activation energies, while the simulation data justify the inherent assumption of a constant relaxation time prefactor in the RRDM.

References and Notes

- (1) Berthet, J. C.; Saelee, C.; Liang, T.; Nicholson, T. M.; Davies, G. R. *Macromolecules* **2006**, *39*, 8186–8192.
- (2) Hoffman, J. D.; Pfeiffer, H. G. *J. Chem. Phys.* **1954**, *22*, 132–141.
- (3) Hänggi, P.; Talkner, P.; Borkovec, M. *Rev. Mod. Phys.* **1990**, *62*, 251–341.
- (4) Gómez, D.; Alegria, A.; Arbe, A.; Colmenero, J. *Macromolecules* **2001**, *34*, 503–513.
- (5) Cendoya, I.; Alegria, A.; Alberdi, J. M.; Colmenero, J. *Macromolecules* **1999**, *32*, 4065–4078.